Interface Engineering for 25% CdTe Solar Cells

Tursun Ablekim[*]*, Eric Colegrove and Wyatt K. Metzger*

National Renewable Energy Laboratory, Golden, Colorado, 80401, USA

Abstract — Buffer layers such as CdS and $Mg_xZn_{1-x}O$ (MZO) are critical for CdTe and other thin film polycrystalline solar cells. A ternary such as MZO allows for interface engineering by adjusting composition, bandgap, and doping to manipulate barriers and recombination to enhance thin film efficiencies towards 25%. Here, theoretical studies demonstrate the enormous impact front interface offset and emitter doping have on device performance. The results reveal it is possible to achieve 25% device efficiency with open-circuit voltage > 1V, even for 10^5 cm/s recombination velocity, provided the interface offsets and doping are properly engineered.

Key words—Cadmium telluride, CdTe, $Mg_xZn_{1-x}O$, thin film solar cells, recombination

The maximum solar cell efficiency and open-circuit voltage (Voc) are determined by the bandgap predicted by the detailed-balance limit [1]. For CdTe solar cells, the theoretical efficiency and Voc limits are ~30% and ~1.2 V, respectively [1]. Experimental record cells have reached ~22% [2], leaving significant room for improvement. Record short-circuit current density (Jsc) is > 30 mA/cm^2 and near its theoretical limit, but corresponding Voc remains between 800- 900 mV [3-4]. Using highly p-type single crystal CdTe absorbers in an otherwise traditional polycrystalline solar cell film stack, the National Renewable Energy Laboratory (NREL) reported Voc >1 V [5] and

transferring the knowledge into industrially manufacturable poly-crystal (PX) thin films is ongoing.

Polycrystalline CdTe have traditionally been limited to hole density on the order of 10^{14} cm^{-3}, and high carrier recombination exists at the absorber and interfaces. The glass/TCO/buffer/absorber configuration combines amorphous, nanocrystalline, and polycrystalline layers with different bandgaps that should create defect, strain, band alignment, and recombination issues [5].

For these reasons, CdS was used as a standard buffer layer between CdTe and TCO because it produced reasonable overall attributes and efficiency despite its disadvantage in collecting the blue (<500 nm) solar spectrum region. Recently, $Mg_xZn_{1-x}O$ (MZO) has showed advantages over CdS, such as large bandgap (preferred for a buffer layer) and a conduction band that can be adjusted with Mg composition. Colorado State University recently demonstrated successful integration of MZO into devices with 19% cell efficiency [6-7]. However, no other institutions have publicly reported successful MZO integration. As parallel efforts increase absorber hole density to > 10^{16} $cm^{-3,}$ the impact of emitter doping, and interface recombination will become more critical. Engineering the interface with materials such as MZO will become as critical to extending efficiency to >25% as improving the absorber material properties [8]. While ideally interface recombination may be reduced to ~0 cm/s in the future, it is also plausible that recombination velocities on the order of 10^5 cm/s will remain, and/or a combination of interface engineering and recombination reductions will be required for next generation efficiency. In this work, we present numerical simulations investigating the impact of doping in CdTe, MZO and the offset at the front

interface on device performance to help guide future research efforts to achieve > 25% efficiency in CdTe based solar cells.

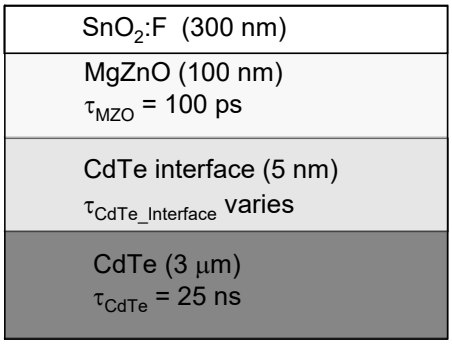

Figure 1. Device film stack used in simulations.

Simulations were performed by simultaneously solving the diffusion and electron/hole continuity equations using the Sentaurus device software [9] assuming the device stack shown in Figure 1. The MZO bandgap was set to 3.64 eV. The thickness of MZO layer was 100 nm with electron and hole lifetimes of 100 ps [10]; varying the MZO lifetimes showed minimal impact on device performance (not shown). Rather than relying on an infinitesimal interface line model and one node driving critical interface physics, a 5-nm CdTe layer is introduced adjacent to the MZO to account for interface states and recombination. The interface electron and hole lifetimes were varied together to 5, 50 and 500 ps, which translate into surface recombination velocities of $S = 1 \times 10^5$, 1×10^4, 1×10^3, cm/s, respectively. The CdTe bulk lifetime was set to 25 ns. Hole and electron densities for MZO and CdTe were varied along with MZO electron affinities to examine the effect of possible achievable values on performance. The MZO electron affinity (χ) varied between 4.1 eV and 4.8 eV, while bulk CdTe was maintained fixed at 4.4 eV. To focus just on the MZO/CdTe affinity effects here, the TCO affinity was tied to the MZO affinity. The changes in χ of MZO result in conduction band offset (ΔE_C) with CdTe. The offset between MZO and CdTe were determined by $\Delta E_C = \chi$ (CdTe) – χ (MZO), so χ variations of MZO between 4.1 to 4.8 eV result in

ΔE_C varying from 0. 3 eV to -0.4 eV, where the positive and negative offsets refer to "spike" and "cliff", respectively. The simulations assume no grain boundary recombination and an ohmic back barrier to focus on front interface effects on device performance. Other material parameters used in the simulations were consistent with past work [8].

First, we studied the impact of doping in the emitter and absorber. Figure 2 shows the impact of absorber and emitter carrier density along for conduction band offset variations representing a 1) a 0.2-eV spike, 2) 0.0 eV offset and 3) a 0.2-eV cliff.

For the 0.2-eV spike and low CdTe hole density (< mid-10^{15} cm^{-3}), MZO electron density does not significantly impact device performance. As CdTe hole density increases, MZO electron density becomes increasingly important. When CdTe hole density reaches mid-10^{16} cm^{-3}, the MZO electron density needs to be > 10^{18} cm^{-3} to achieve ~25% efficiency. If low-electron density MZO is used with highly p-type CdTe, device performance drops quickly to near 1-5% in part from a significant loss in FF and Jsc. Interface recombination is related to the number of available holes and electrons flowing into the interface, and *S*, the interface recombination velocity. When there is a positive conduction band offset ("spike"), there is band bending in the conduction band minimum (E_c) near the interface towards the quasi-fermi level of electrons (E_{Fn}), which forces the interfacial CdTe valence band maximum (E_v) downward, creating a larger barrier for holes entering the interface. A cliff introduces less band banding followed by a smaller barrier for the holes allowing for a large hole density entering the interface, enhancing recombination [11].

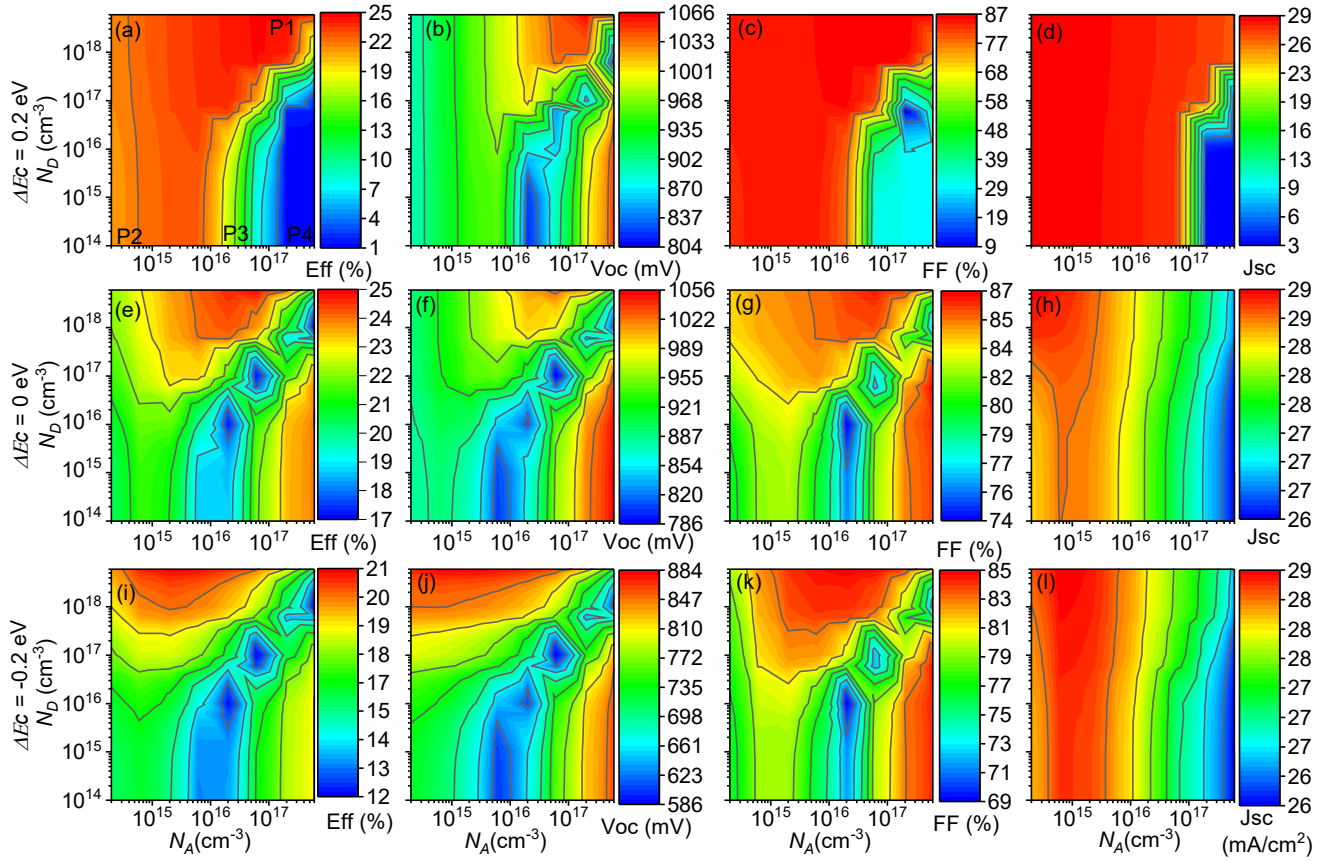

Figure 2. Simulated contour plots of device performance parameters (efficiency, Voc, FF and Jsc) with electron concentrations in MZO (N_D) and hole concentration in CdTe (N_A) for a 0.2-eV spike (top, figures a-d), 0-eV flat band (middle, figures e - h) and -0.2-eV cliff (bottom, figures i - l). The surface recombination velocity for both plots are $S = 10^5$ cm/s.

The band bending is also related to the emitter and absorber carrier concentrations. Figure 3 shows JV plots, band diagrams, and recombination plots from four N_A and N_D values (labeled with P1 – P4) from the Figure 2 (a) plot for a 0.2-eV spike. When $N_D > N_A$ as in P1, the potential drop mostly occurs in the CdTe, leading to large band bending and larger hole barriers. When CdTe carrier concentration is greater than MZO as in P3 and P4, the potential drops more in the MZO side, allowing for larger number of holes flowing into the interface, enhancing recombination.

Figure 3(c) shows the recombination rate (R_{IF}) at the interface, where the R_{IF} increases by five orders of magnitude from P1 to P4.

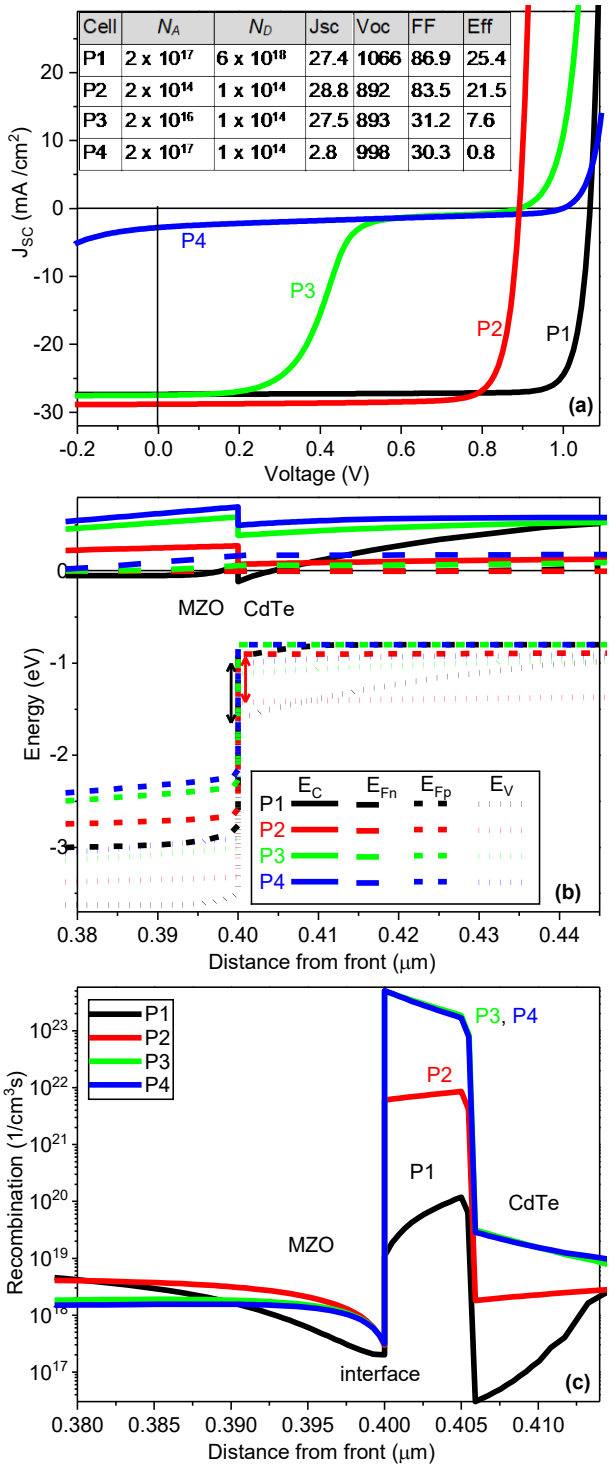

Figure 3. (a) J-V plots of four cells corresponding to four different carrier densities in CdTe and MZO, labeled P1 to P4. The labels correspond to the efficiency plot with ΔE_C = 0.2 eV spike in Figure 2a (b) Band diagram. (c) Recombination at the defective interface region. The distance is calculated from the front surface of TCO.

With a flat conduction band offset (ΔE_C = 0 eV, Figure 2, middle), one still can get 25% efficiency and ~1066 mV Voc, but the window becomes much smaller, limited to when the MZO and CdTe carrier concentrations are orders of magnitude different. When carrier concentrations are similar, the Voc and overall performance decrease

The contour pattern for -0.2 eV cliff (Figure 2, bottom) is similar but achievable maximum device efficiency and voltage drops to 21% and 884 mV, respectively. This is due to the fact that the cliff enhances hole flow into the interface, facilitating the interface recombination.

Strikingly, the device performance can vary dramatically with different carrier concentrations, yet the community does not systematically measure or control these values, particularly after $CdCl_2$ treatments.

Next, we studied the impact of conduction band offset on device performance. The conduction band offset between MZO and CdTe plays a critical role in current collection and Voc. Positive band offset mitigates recombination current enhancing Voc. Figure 4 presents systematic ΔE_C changes with variations in MZO electron density for 2×10^{14} cm^{-3} and 2×10^{16} cm^{-3} CdTe, respectively. The former represents the levels consistent with traditional Cu and Cl defect chemistry, and the latter the levels achievable by Group-V doping [12-13], When CdTe doping is 2×10^{14} cm^{-3} and the ΔE_C is 0.1 eV to 0.3 eV, the impact of MZO electron density on performance is not significant, with Voc ~890 mV and efficiency ranging from 20-22%. When ΔE_C gradually decreases from spike to cliff, Voc loss becomes more pronounced due to enhanced recombination, dropping to less than 600 mV with ΔE_C < -0.3 eV, while the Jsc varies relatively little. When ΔE_C is too large (> 0.4 eV), high Voc above 900 mV is restored due to the large band bending, but the

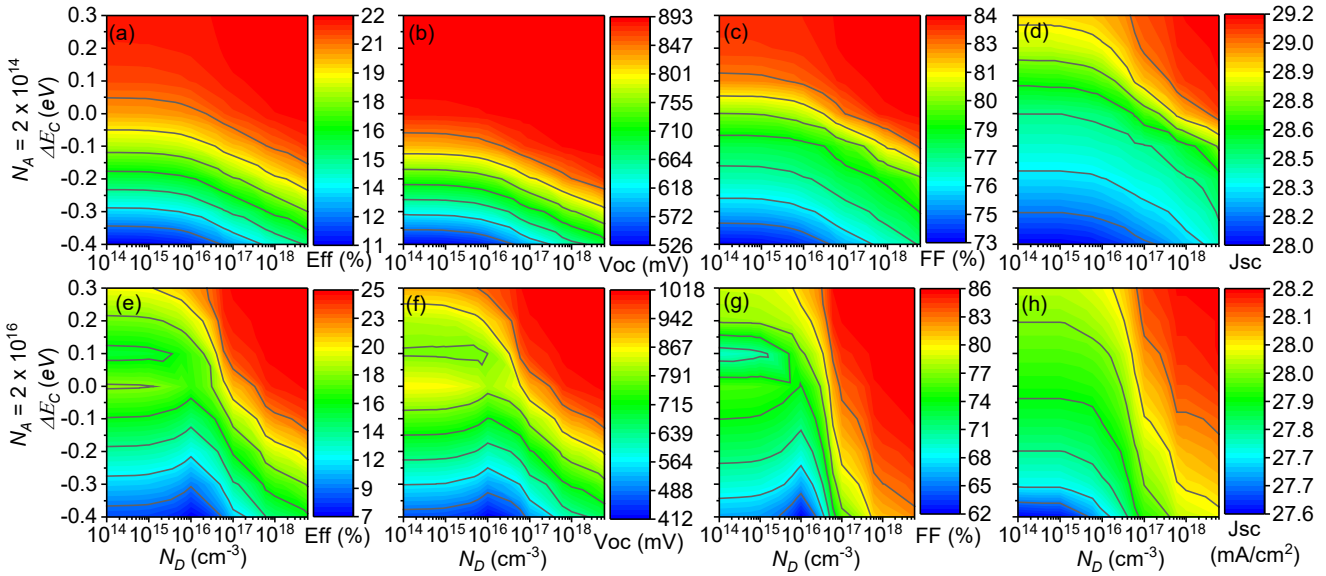

Figure 4. Simulated contour plots of device performance (efficiency, Voc, FF and Jsc) with variations in the conduction band offset (ΔE_C) and electron density (N_D) in MZO for CdTe doping of 2×10^{14} cm^{-3} (top, figures a-d) compared to CdTe doping of 2×10^{16} cm^{-3} (bottom, figures e-h). The interface recombination velocity S is 1×10^5 cm/s for both cases.

large spike adversely effects current collection by blocking current flow, leading to insufficient current collection. More anomalous large spike and cliff situations are not included in the plots.

When CdTe doping increased to 2×10^{16} cm^{-3}, efficiencies of 25% are possible but MZO electron density becomes more important in addition to offset. For example, 25% efficiency with 1000 mV Voc requires MZO electron density > 1×10^{17} cm^{-3} with a spike around 0.1 eV to 0.3 eV at the interface. Again, the Jsc doesn't change much in both CdTe doping.

The impact of surface recombination velocity is also of interest. With a fixed hole and electron density, higher S generally enhances recombination, resulting in a loss in Voc. Figure 5 compares similar efficiency plots to those of Figure 2 and 4 for 10^5, 10^4, and 10^3 cm/s recombination velocities. The general contour patterns remained unchanged, but the windows for high performance naturally tighten. For example, when comparing ΔE_C *vs*. N_D for 2×10^{14} cm^{-3} CdTe doping ΔE_C = 0.05 eV spike or higher is desired for best device performance when $S = 10^5$ cm/s but the tolerance improves to -0.1 eV and -0.15 eV cliffs when S decreases to 10^4 and 10^3 cm/s, respectively. Although the patterns remain similar with variations in S, the lower bound of

achievable efficiency increases with decreasing *S*. For example, low cell performance of 7% in Figure 5b increases to 13% in Figure 5j as *S* shifts from 10^5 to 10^3 cm/s. Importantly, the achievable highest efficiency remains critically tied to CdTe hole density, shifting from ~22% to >25% for $N_A = 2\times10^{14}$ and 2×10^{16} cm^{-3}, respectively, regardless of improvements in surface recombination

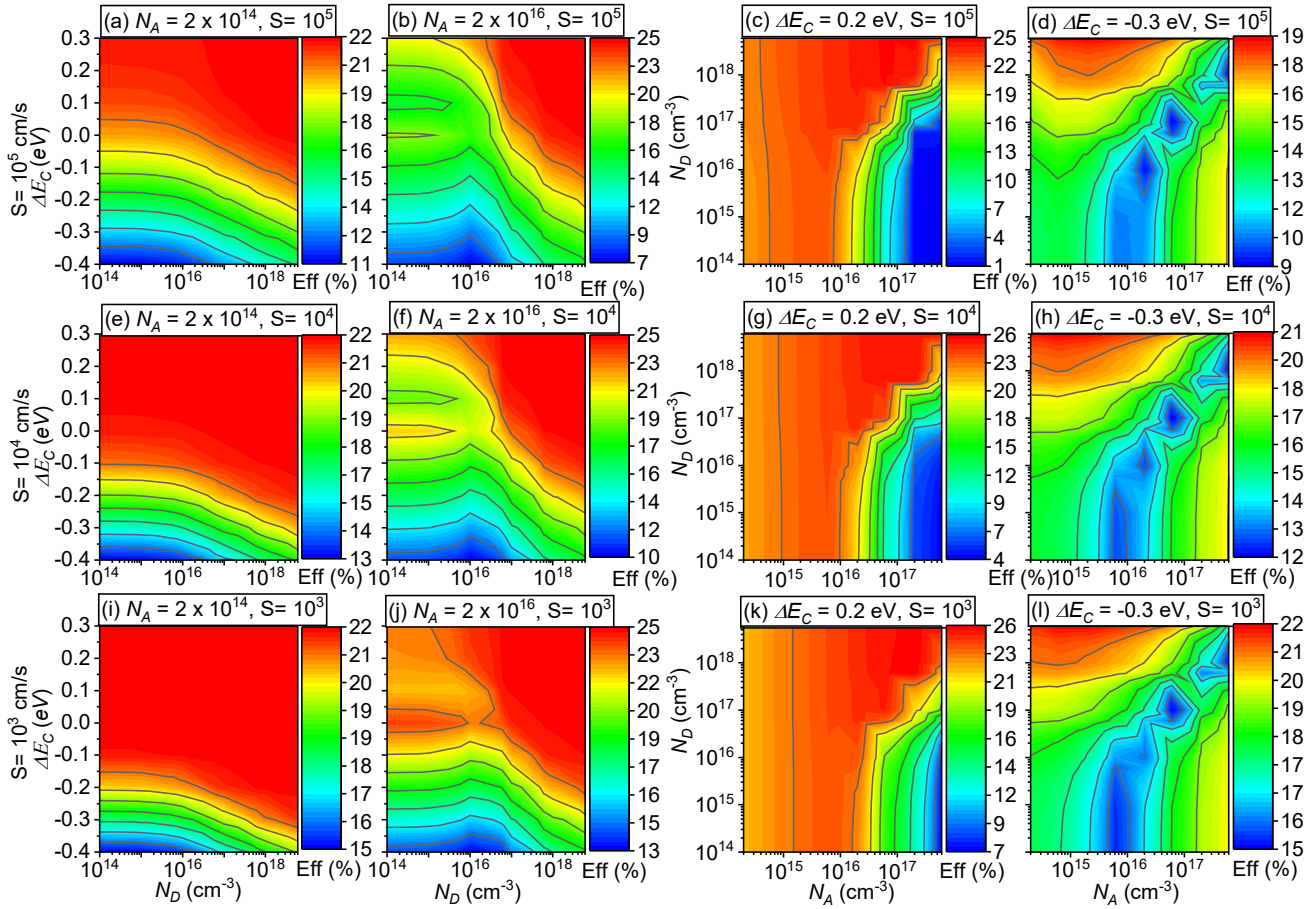

Figure 5. Comparison of simulated efficiency contour plots with variations in the conduction band offset (ΔE_C), electron density in MZO (N_D), CdTe doping (N_A), and interface recombination velocities values (S). S is isolated for each row at 10^5 cm/s (top, figures a-d), 10^4 cm/s (middle, figures e-h), and 10^3 cm/s (bottom, figures i-l). N_A is isolated for the left two columns at 2×10^{14} cm^{-3} (figures a, e and i) and 2×10^{16} cm^{-3} (figures b, f, and j) for each ΔE_C *vs.* N_D plot. ΔE_C is isolated for the right two columns at 0.2 eV (spike, figures c, g, and k) and -0.3 eV (cliff, figures d, h, and l) for each N_D *vs.* N_A plot.

By systematically investigating the impact of interfacial band alignment and MZO and CdTe carrier concentrations for different interface recombination velocities, we find that interface engineering will be critically important to achieve next-generation efficiencies. As Group-V dopants increase N_A, the impact of emitter doping is more important, so it is important to measure.

In addition to attempting to reduce *S*, adjusting the emitter doping will be important. Furthermore, manipulating the emitter band alignment and measuring these properties after $CdCl_2$ treatment in completed devices will become necessary and is currently not done by CdTe community or thin film communities in general. MZO represents one material to adjust alignment, electron density, and passivation [14], but others, including CTO, ZTO, and SnO_2, may provide other paths to engineer thin film interfaces in the futures. This work provides a guide to the critical features and paths.

AUTHOR INFORMATION

Corresponding Author

Email: tursun.ablekim@nrel.gov

Author Contributions

The manuscript was written through contributions of all authors. All authors have given approval to the final version of the manuscript.

Funding Sources

Funding for this work is provided by U.S. Department of Energy Office of Energy Efficiency and Renewable Energy Solar Energy Technologies Office

Notes

The authors declare no competing financial interest.

ACKNOWLEDGEMENT

This work was authored by Alliance for Sustainable Energy, LLC, the manager and operator of the National Renewable Energy Laboratory for the U.S. Department of Energy (DOE) under Contract No. DE-AC36-08GO28308. Funding provided by U.S. Department of Energy Office of

Energy Efficiency and Renewable Energy Solar Energy Technologies Office. The views expressed in the article do not necessarily represent the views of the DOE or the U.S. Government. The U.S. Government retains and the publisher, by accepting the article for publication, acknowledges that the U.S. Government retains a nonexclusive, paid-up, irrevocable, worldwide license to publish or reproduce the published form of this work, or allow others to do so, for U.S. Government purposes.

REFERENCES

1. Rühle, S., Tabulated values of the Shockley–Queisser limit for single junction solar cells. *Solar Energy* **2016,** *130*, 139-147.

2. Solar, F. First Solar Achieves Yet Another Cell Conversion Efficiency World Record. http://investor.firstsolar.com/news-releases/news-release-details/first-solar-achieves-yet-another-cell-conversion-efficiency; last accessed Aug 30 2018.

3. Gloeckler, M.; Sankin, I.; Zhao, Z., CdTe Solar Cells at the Threshold to 20% Efficiency. *IEEE Journal of Photovoltaics* **2013,** *3* (4), 1389-1393.

4. Green, M. A.; Hishikawa, Y.; Dunlop, E. D.; Levi, D. H.; Hohl-Ebinger, J.; Ho-Baillie Anita, W. Y., Solar cell efficiency tables (version 51). *Progress in Photovoltaics: Research and Applications* **2018,** *26* (1), 3-12.

5. Burst, J. M.; Duenow, J. N.; Albin, D. S.; Colegrove, E.; Reese, M. O.; Aguiar, J. A.; Jiang, C. S.; Patel, M. K.; Al-Jassim, M. M.; Kuciauskas, D.; Swain, S.; Ablekim, T.; Lynn, K. G.; Metzger, W. K., CdTe solar cells with open-circuit voltage breaking the 1 V barrier. *Nature Energy* **2016,** *1*, 16015.

6. Munshi, A. H.; Kephart, J.; Abbas, A.; Raguse, J.; Beaudry, J. N.; Barth, K.; Sites, J.; Walls, J.; Sampath, W., Polycrystalline CdSeTe/CdTe Absorber Cells With 28 mA/cm^2 Short-Circuit Current. *IEEE Journal of Photovoltaics* **2018,** *8* (1), 310-314.

7. Munshi, A. H.; Kephart, J. M.; Abbas, A.; Shimpi, T. M.; Barth, K. L.; Walls, J. M.; Sampath, W. S., Polycrystalline CdTe photovoltaics with efficiency over 18% through improved absorber passivation and current collection. *Solar Energy Materials and Solar Cells* **2018,** *176*, 9-18.

8. Kanevce, A.; Reese, M. O.; Barnes, T. M.; Jensen, S. A.; Metzger, W. K., The roles of carrier concentration and interface, bulk, and grain-boundary recombination for 25% efficient CdTe solar cells. *Journal of Applied Physics* **2017,** *121* (21), 214506.

9. Synopsys, TCAD SDEVICE Manual. Zurich, Switzerland. www.synopsys.com; last accessed Aug. 30 2018.

10. Amarasinghe, M.; Colegrove, E.; Moseley, J.; Moutinho, H.; Albin, D.; Duenow, J.; Jensen, S.; Kephart, J.; Sampath, W.; Sivananthan, S.; Al-Jassim, M.; Metzger, W. K., Obtaining Large Columnar CdTe Grains and Long Lifetime on Nanocrystalline CdSe, MgZnO, or CdS Layers. *Advanced Energy Materials* **2018,** *8* (11), 1702666.

11. Song, T.; Kanevce, A.; Sites, J. R., Emitter/absorber interface of CdTe solar cells. *Journal of Applied Physics* **2016,** *119* (23), 233104.

12. Burst, J. M.; Farrell, S. B.; Albin, D. S.; Colegrove, E.; Reese, M. O.; Duenow, J. N.; Kuciauskas, D.; Metzger, W. K., Carrier density and lifetime for different dopants in single-crystal and polycrystalline CdTe. *APL Materials* **2016,** *4* (11), 116102.

13. Colegrove, E.; Yang, J. H.; Harvey, S. P.; Young, M. R.; Burst, J. M.; Duenow, J. N.; Albin, D. S.; Wei, S. H.; Metzger, W. K., Experimental and theoretical comparison of Sb, As, and P diffusion mechanisms and doping in CdTe. *Journal of Physics D: Applied Physics* **2018,** *51* (7), 075102.

14. Kephart, J. M.; McCamy, J. W.; Ma, Z.; Ganjoo, A.; Alamgir, F. M.; Sampath, W. S., Band alignment of front contact layers for high-efficiency CdTe solar cells. *Solar Energy Materials and Solar Cells* **2016,** *157*, 266-275.

TOC